Power-law estimation of branch growth

Kaitaniemi, Pekka

2020-01-15

Kaitaniemi , P , Lintunen , A & Sievanen , R 2020 , ' Power-law estimation of branch growth ' , Ecological Modelling , vol. 416 , 108900 . https://doi.org/10.1016/j.ecolmodel.2019.108900

http://hdl.handle.net/10138/313017
https://doi.org/10.1016/j.ecolmodel.2019.108900

Ecological Modelling 416 (2020) 108900

Contents lists available at ScienceDirect

Ecological Modelling

journal homepage: www.elsevier.com/locate/ecolmodel

Power-law estimation of branch growth

Pekka Kaitaniemi[a,*], Anna Lintunen[b,c], Risto Sievänen[d]

[a] Hyytiälä Forestry Field Station, Faculty of Agriculture and Forestry, University of Helsinki, Hyytiäläntie 124, FI-35500, Korkeakoski, Finland
[b] Institute for Atmospheric and Earth System Research / Physics, Faculty of Science, P.O. Box 64, FI-00014, University of Helsinki, Finland
[c] Institute for Atmospheric and Earth System Research / Forest Sciences, Faculty of Agriculture and Forestry, P.O. Box 27, FI-00014, University of Helsinki, Finland
[d] Natural Resources Institute Finland (Luke), P.O. Box 2, FI-00791, Helsinki, Finland

ARTICLE INFO

Keywords:
Allometry
Crown structure
Spatial interactions
S-systems
Structural parameters

ABSTRACT

We demonstrate the efficacy of power-law models in the analysis of tree branch growth. The models can be interpreted as allometric equations, which incorporate multiple driving variables in a single scaling relationship to predict the amount of growth within a branch. We first used model selection criteria to identify the variables that most influenced (1) the length of individual elongating annual shoots and (2) the total length of all elongating annual shoots in the individual branches of silver birch (*Betula pendula* Roth). We then applied the two resulting power-law equations as dynamic models to predict the trajectories of crown profile development and accumulation of branch biomass during tree growth, using total branch length as a proxy for biomass. In spite of the wide size range and geographical distribution of the study trees, the models successfully reproduced the dynamic characteristics of crown development and branch biomass accumulation. Applying the model to predict long-term growth of a single branch that was initiated at the crown top generated a realistic crown profile and produced a final basal branch size that was well within the range of field observations. The models also predicted a set of more subtle and non-trivial features of crown formation, including the increased rate of growth towards the tree apex, decrease in growth towards the lowest branches, the effect of branching order on the amount of elongation, and the higher vigour of thick branches when the effect of branch height was controlled. In contrast, a simple allometric model of the form $Y = aX^b$ was incapable of capturing all the variability in growth of individual branches and of predicting the features of crown shape and branch size that are associated with the slowing-down of growth towards the crown base. We conclude that power-law models where the parameter a is refined to include spatial information on branch features shows good potential for identifying and incorporating actual crown construction processes in dynamic models that utilize the structural features of tree crowns.

1. Introduction

Development of tree crown is an iterative process in which a tree constantly grows to adjust the three-dimensional (3D) structure in response to changes in the environment and the internal organization (Sorrensen-Cothern et al., 1993; Pretzsch, 2014). Although crown construction averaged over several tree species largely follows allometric laws and other biophysical rules (Farnsworth and Niklas, 1995; Enquist, 2002; Bejan et al., 2008), there remains ample variation within and between species and individuals (Lines et al., 2012; Bentley et al., 2013; Pretzsch, 2014).

A seemingly stochastic component is involved in within-crown distribution of extension growth within branches (Buck-Sorlin, 2000; Stevenson et al., 2000; Kull and Tulva, 2002; Koyama et al., 2017). A wide variety of environmental factors can generate apparent stochasticity in crown development, because they influence local growth habits and generate plastic responses. Environmental factors include the quantity and quality of light (Baraldi et al., 1994; Kukk and Sõber, 2015), wind and gravity (Brüchert and Gardiner, 2006; James et al., 2006), mechanical contacts with neighbours (Hajek et al., 2015), availability of growing space (Simard and Zimonick, 2005), temperature (Nakamura et al., 2016) and activities of other organisms (Haukioja et al., 1990; Gonda-King et al., 2014).

The internal organization of a crown comprises multiple organs and tissues competing for limited resources. Allocation among the competing sites is affected by concurrent physical and ecophysiological factors that include hormonal control and correlative inhibition (Sprugel, 2002; Tworkoski et al., 2006), trade-offs among elongation, radial growth and reproduction (Obeso, 1997; Kramer et al., 2014), biomechanical requirements (Sone et al., 2006; Loehle, 2016), capacity

* Corresponding author.
E-mail address: pekka.j.kaitaniemi@helsinki.fi (P. Kaitaniemi).

https://doi.org/10.1016/j.ecolmodel.2019.108900
Received 19 June 2019; Received in revised form 21 November 2019; Accepted 21 November 2019
Available online 05 December 2019

of transport tissue (Grönlund et al., 2016) and hydraulic limits (Koch et al., 2004).

Several studies of trees have reported consistencies between annual elongation and internal and external factors under strictly controlled growth conditions (Normand et al., 2009; Chen and Sumida, 2017), in tree saplings (Messier and Nikinmaa, 2000; Takahashi et al., 2006, Collet et al., 2011), and in fixed crown positions (Osada et al., 2014). The generation of crown asymmetry is well documented, and the importance of hierarchical branching order for shoot growth is also well known (Jones and Harper, 1987; Young and Hubbell, 1991; Lintunen et al., 2011). However, the information available on within-crown patterns of branch growth is scattered, and spatially and ontogenetically limited, because typical studies cover growth at specific crown positions of only a handful of trees growing at a single site. In ecological interactions that shape the competitive success of individual trees, the functioning of plastic growth patterns within the crown thus remains largely unexplored (Ford, 2014). Even the process-based functional-structural models of tree architecture frequently simplify representation of resource allocation to branches, using growth rules that overlook the identification of the actual processes that generate crown architecture (Lacointe, 2000; Mathieu et al., 2009; Ford, 2014).

Here, we focus on the analysis of branch growth throughout the entire crowns of silver birch (*Betula pendula* Roth) individuals ranging from the juvenile to the reproductive stage within a geographical gradient. Our aim is to identify the best set of explanatory variables for dynamic models that encompass the patterns of branch growth shared by the tree individuals regardless of the developmental stage or the effects of unknown site-specific factors. We considered both structural variables and variables that estimated the availability of photosynthetic radiation, as well as plausible proxies for physiological information. As an advancement to our previous analyses of static crown structure (Lintunen and Kaitaniemi, 2010; Lintunen et al., 2011), we demonstrate the use of power-law models as a method that serves both to detect the dominant factors influencing branch growth within the crown and as a method for constructing dynamic models to estimate branch growth and crown formation.

2. Materials and methods

2.1. Power-law modelling

The power-law models can be considered as allometric scaling equations ($Y = aX^b$) in which the normalization constant *(a)* has been modified to include information on additional factors affecting the scaling relationship, a procedure that has been implicitly adopted in many existing model equations (e.g. Cole and Lorimer, 1994; Mäkinen, 2002; Kantola and Mäkelä, 2004), and explicitly considered in others (White and Gould, 1965; Kaitaniemi and Lintunen, 2008; Peters et al., 2018).

We analysed branch growth within the crown of silver birch by focusing on annual branch elongation rate described as 1) the annual total branch elongation (ΔL_b), calculated as the summed length of all elongating shoots within individual first-order branches, and 2) the annual length of the individual elongating shoots (ΔL_s). The models for ΔL_b and ΔL_s were constructed as power-law models, imitating the S-system approach (Voit, 2000), as:

$$\Delta L_j = \alpha X_1^{g1} X_2^{g2} X_3^{g3} \ldots X_i^{gi} \qquad j = b \text{ or } s, \tag{1}$$

where X_i are independent explanatory variables, α and g_i are parameters, and $j = b$ refers to the model of ΔL_b and $j = s$ to the model of ΔL_s.

Using branch diameter (d_b) as an example of an explanatory variable (X^{gi}), the Eq. (1) can be interpreted as an allometric equation with the form

$$\Delta L_j = a d_b^{gi} \qquad j = b \text{ or } s \tag{2}$$

where g_i is the scaling exponent and a is the normalization constant following from Eq. (1) as

$$a = \alpha X_1^{g1} X_2^{g2} X_3^{g3} \ldots X_{i-1}^{gi-1} \tag{3}$$

The construction of power-law models is not restricted to structural features, which are widely used for the static allometric analysis of tree structure by utilizing logarithmically transformed versions of power-law equations (Sileshi, 2014). Variables describing the contribution of physiological processes can be equally included in the list of independent explanatory variables (X_i) as long as their values can be considered constant at the time scale when the value of the dependent response variable (such as ΔL_j here) is set (Voit and Sands, 1996). Yet, the potential of power-law models to operate as dynamical models of plant development by themselves has remained largely unexplored, with few examples covering the dynamic processes of tree growth (Voit and Sands, 1996; Renton et al., 2005a,b). In other contexts, the S-system approach with its power-law notation has been documented extensively with plentiful justification for process modelling (Savageau, 1979a,b; Voit, 2000; Voit et al., 2015).

2.2. Variables for models of branch elongation in silver birch

We considered a selected set of structural and physiological variables to potentially influence branch growth in silver birch (Fig. 1, Table 1). We first used a full set of candidate variables to construct models according to Eq. (1), and then used model selection criteria to identify the most parsimonious set of variables to remain as independent variables X_i. One year was used as the time step to calculate ΔL_j and to estimate the values of X_i. Branch-specific values were used for ΔL_b, and values specific for an individual long shoot (Fig. 1) were used for ΔL_s as described in Table 1.

The annual levels of PAR and N_{area} were included as potential X_i variables, because both have been associated with crown growth habits

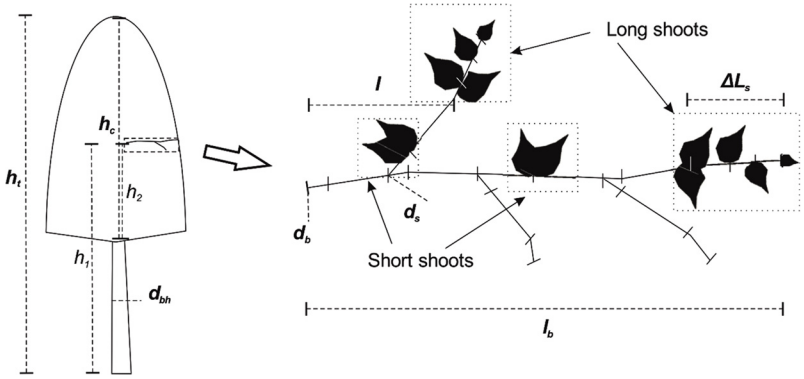

Fig. 1. Measurement and calculation of structural branch parameters listed in Table 1. $h_{rt} = h_1/h_t$, where h_1 is the height of the branch base and h_t is the total tree height. $h_{rc} = h_2/h_c$, where h_2 is the distance between the branch base and the lowest living branch and h_c is the crown length. $l_{rb} = l/l_b$, where l is the distance between the shoot base and the branch base along the line l_b, and l_b is the primary branch axis length measured as a straight line between the branch base and tip. d_{bh} is diameter at breast height, d_b is the primary branch base diameter and d_s diameter at the bifurcation point of the side branch bearing a long shoot. In silver birch, the long shoots are responsible for elongation and production of new buds whereas the short shoots bear only one bud and typically elongate less than 5 mm per year. The short lines (|) crossing the branch indicate typical points of recording information during the measurement of branch structure. The downward facing side branches have been drawn without foliage.

Table 1
List of the explanatory variables considered. See Fig. 1 for explanations. PAR refers to the relative amount of photosynthetically active radiation estimated under an overcast sky.

Variable	Unit	Description
a) *Model for total branch elongation (ΔL_b)*		
PAR_{av}		branch-specific average PAR
h_{rt}		height of primary branch base in relation to tree height
h_{rc}		height of primary branch base in relation to crown length
$l_{rb,\ av}$		branch-specific average relative distance of long shoots from branch base along the main axis
d_b	cm	primary branch base diameter
$d_{s,\ av}$	cm	branch-specific average of side branch diameter at bifurcation points within a branch
d_{bh}	cm	tree diameter at breast height
$N_{area,\ av}$	g m^{-2}	branch-specific average of area-based nitrogen content of foliage within a branch
l_{bn}	cm	tree-specific average distance of basal branches to neighbouring tree branches
b) M*odel for individual long shoot elongation (ΔL_s)*		
PAR[a]		relative amount of photosynthetically active radiation under overcast sky
h_{rt}		height of primary branch base in relation to tree height
h_{rc}		height of primary branch base in relation to crown length
l_{rb}		relative distance of long shoot from branch base along the primary branch axis
d_b	cm	primary branch base diameter
d_s	cm	diameter at the bifurcation point of the side branch bearing the long shoot
d_{bh}	cm	tree diameter at breast height
N_{area}[a]	g m^{-2}	area-based nitrogen content of foliage
l_{bn}	cm	tree-specific average distance of basal branches to neighbouring tree branches

[a] Sampled within a cube with 20 cm side lengths around the shoot base.

in different studies (Umeki and Seino, 2003; Dong et al., 2015, Coble et al., 2017). PAR and PAR_{av} (Table 1) indicate the potential to capture photosynthates, and N_{area} indicates the availability and distribution of a key nutrient that also itself is related to the photosynthetic potential within the crown (Evans, 1989; Wyka et al., 2016). Although the values of PAR and PAR_{av} correlate with N_{area}, their relationship in silver birch is not straightforwardly linear, which leaves open the possibility of partially independent effects (Kaitaniemi et al., 2018).

The availability of growing space and the risk of mechanical abrasion within the stand are also both known to influence growth allocation (Young and Hubbell, 1991; Hajek et al., 2015), and their potential effects were included in the models using l_{bn} to indicate the proximity of neighbouring trees.

The variables d_b, d_s, and d_{bh}, or variables closely related to them, are standard variables in models of plant development, and their influence on elongation growth can be linked to both structural allometry and transport capacity within a tree (Ford et al., 1990; Grote and Pretzsch, 2002; Savage et al., 2010). d_{bh} also serves to indicate the age and ontogenetic stage of a tree.

The annual values of the variables h_{rt}, h_{rc}, and l_{rb}, in turn, represented the variants of positional variables, which have turned out successful in characterizing many patterns of tree growth (Baldwin and Peterson, 1997; Grote and Pretzsch, 2002; Remphrey et al., 2002, Renton et al., 2006; Normand et al., 2009). They can be considered as aggregate variables that potentially contain information on many types of processes. For example, they are, to some extent, linked with the distribution of PAR within the silver birch crown (Kaitaniemi et al., 2018), but may also reflect various features of internal organization in terms of the relative transport capacity for nutritive, hormonal or other substances within the stem, crown or individual branch (Sachs, 2004). In the analysis of ΔL_b, their average values also reflected structural constraints stemming from previous growth events.

We excluded branch mortality and other types of resource loss, due to the lack of substantial data, and likewise did not consider the numbers of buds produced within branches.

Table 2
Numbers of sample trees in various diameter classes.

Diameter range (d_{bh}, cm)	N of trees
4 – 8	6
8 – 12	16
12 – 16	5
16 – 20	5

2.3. Data for model calibration

The data for the calibration of the branch growth models originated from eight study plots with two to six trees each (N = 32 trees in all), and were a subset of the data described in further detail in Table 1 from both Kaitaniemi and Lintunen (2010) and Lintunen and Kaitaniemi (2010). The sample trees had either Scots pine (*Pinus sylvestris* L.) or silver birch as the dominant neighbouring species. Already existing architectural models were used in the estimation of PAR and PAR_{av} for these two species (Kaitaniemi et al., 2018). The 4 – 35-year-old study trees were in the phase of active growth and covered a wide size range (Table 2). The study plots were located along a 400-km southwest-northeast transect between latitudes 60 °N and 63 °N and longitudes 21 °E and 29 °E in the boreal forest zone of Finland and represented *Myrtillus* type forest sites, characterized by mesic till soils and medium fertility.

Annual elongation through the growth of long shoots was measured to describe the rate of elongation in each study branch (ΔL_s and ΔL_b). Elongation was measured at the end of the growing season from a sample of 1–12 sample branches systematically selected from the basal, middle and apical part of each tree crown. On average there were six sample branches per tree. ΔL_s was measured as the distance between the long shoot base and the most apical bud of a long shoot, and ΔL_b was calculated as the sum of all individual long shoot lengths within a branch (Fig. 1).

The ΔL_s values for each long shoot position were obtained, along with the full 3D structure of the sample branches, by recording the 3D positions of all individual short and long shoots and branching points using a digitizer in the field (Fig. 1, Lintunen and Kaitaniemi, 2010). Dead side branches were left out from the measurements. The procedure provided also the 3D positions of the sample branches within the main stem. The branching orders (i) and the lengths of branch segments between the long shoot positions were also recorded, which yielded positional information for model development (Fig. 1). In addition to the detailed measurements of the sample branches, the length l_b and branching angle for all the remaining branches of each tree was measured using the digitizer (Lintunen et al., 2011).

Within each sample branch, N_{area} and relative PAR were estimated for one to two foliage sampling positions depending on branch size. Leaf samples for the determination of N_{area} in the lowest crown parts mainly originated from the nonelongating short shoots, whereas the samples in the uppermost parts frequently included two fully expanded basal leaves of elongating long shoots. The leaf area was measured digitally from fresh samples, and the amount of N was analysed from dried samples with the Kjeldahl method. PAR was estimated for the leaf sampling positions (Kaitaniemi et al., 2018), using the LIGNUM model as described in Lintunen et al. (2013). The instantaneous relative PAR with respect to the PAR of an open overcast sky was used as a shortcut estimate of the annual cumulative PAR (Gendron et al., 1998; Yoshimura and Yamashita, 2014).

In order to estimate PAR for the positions of leaf samples, the 3D crown structure with leaves of all trees on the plot was constructed using the models described in Lintunen et al. (2011). If the sampling

position was located inside the canopy, PAR was computed for a total of four random positions within a cube with 20 cm side lengths around the sampling point, and the average of the values was used in the analyses to even out the fine scale variation of light in the crown (Kaitaniemi et al., 2018). Branch-specific average values of relative PAR (PAR_{av}) and N_{area} ($N_{area,\ av}$) were used for the analysis of ΔL_b, whereas the analysis of ΔL_s included only those long shoots (on average nine long shoots per tree) for which measurements of N_{area} and PAR were available within the same 20-cm cube where their basal point was located (Kaitaniemi et al., 2018).

Branch base diameter d_b was measured at the base of each primary branch axis, and diameters (d) for the remaining branch parts, including d_s, were estimated with a taper model (coefficient of determination $R^2 = 0.96$) based on unpublished measurements collected during the study by Lintunen (2013):

$$d = 0.3^{(i-1)}(1 - 0.98\ l_{rb})\ d_b \quad (4)$$

where i is the branching order, such that for the primary branch $i = 1$, for side branches bifurcating from the primary branch $i = 2$, and so on. In the estimation, we assumed that the minimum acceptable diameter was 0.15 cm.

The minimum distance between the tips of the longest branches and the branches of each crown-bordering neighbour tree was measured in four 90-degree compass sectors to obtain tree-specific average distance of basal branches to neighbouring tree branches (l_{bn}). The average of l_{bn} was used for all branches and all long shoots within branches. The measurements of l_{bn} were restricted to neighbouring trees with stems within a 5-m radius from the target tree stem.

2.4. Model selection

We first parameterized the model in Eq. (1) for both ΔL_b and ΔL_s with all the candidate explanatory variables (Table 1) included, and then proceeded with backward elimination of the variables that did not contribute to the model fit. Occasionally, when elimination occurred between two almost equally important variables, the variables eliminated were added back at a later stage to ensure that the contribution of a particular variable was not dependent on other variables remaining in the model. Model selection and parameterization was conducted using the SAS procedure NLMIXED (SAS Institute Inc., Cary, NC, USA) with the Newton-Raphson method with line search as the optimization method. Normal distribution was set as the conditional distribution for the dependent variables ΔL_b and ΔL_s (Wolfinger, 1999). Random effects were not considered because the focus was on the selection of fixed explanatory variables and their parameterization. The Bayesian information criterion (BIC) was used as the criterion for model selection (Schwarz, 1978). The steps of model selection are shown in Appendix A.

2.5. Model validation and analysis

We utilized model-predicted trajectories of long-term branch elongation, and the resulting estimates of crown profile and branch biomass, to validate the behaviour of the final models against three sources of additional data. In the validation, we assumed that the total branch length (L_t) at any time step was suitable as a proxy for branch biomass. The details of calculating the crown profile and the trajectories of growth using the models of ΔL_b and ΔL_s are described in Appendix A.

The first source of data for validation was the model of proportional branch biomass growth by Tahvanainen and Forss (2008), which provided an independent estimate of branch biomass increment over time in different crown positions. We repeatedly applied the model of ΔL_b to generate a similar trajectory of biomass increment as Tahvanainen and Forss (2008). The trajectory of growth was obtained by using the final model of ΔL_b to predict the growth of a single branch initiated at the crown top.

The second source of data was the L_t of the sample branches, which was also obtained during the digitization of the 3D branch structure (Fig. 1). The measured L_t provided estimates of L_t at different crown positions and that way reflected the prior trajectory of total branch elongation (ΔL_b) in the field. To validate the final model of ΔL_b, the average field-measured L_t was compared with L_t predicted by the model at different crown positions during the crown development, similar to the estimation of the biomass growth trajectory.

The third source of data were the lengths (l_b, Fig. 1) of the remaining branches in our study trees, i.e. those branches that were not used for model parameterization, to estimate the average crown profile of the study trees. To obtain a model-predicted crown profile for comparison, the model of ΔL_s was repeatedly applied to predict the branch main axis length (L_c) at each annual time step and crown position. Because the model of ΔL_s predicted L_c, whereas l_b in the data underestimated L_c by ignoring curves within a branch (Fig. 1), the crown profile for comparison was generated from l_b by estimating $L_c = 1.18 l_b$ (see Appendix A for more details). For simplicity, because the crown profile was obtained as a by-product of comparing the model predicted and observed branch lengths during the crown development, we assumed a constant 45° branching angle and a linear shape for all branches in the comparison. Description of a more accurate crown profile estimation for silver birch is available in Lintunen et al. (2011).

Finally, a more detailed analysis of model behaviour in the various crown parts and in trees with differing size was obtained graphically by plotting the outcomes of altering the values of X_i within a representative range.

2.6. Alternative models

The performance of the final models of ΔL_s and ΔL_b was further assessed by comparing them with alternative models obtained from the literature. The fit of the alternative models was compared with the measured ΔL_s and ΔL_b using the same model diagnostics as with the power-law models. In addition to BIC, the fit was assessed by analysing the regression between the observed vs. the predicted values and testing the significance of slope $b = 1$ and intercept $a = 0$ (Piñeiro et al., 2008). The root-mean-squared error (RMSE) was also reported for the alternative models. Further, the fit was also assessed by using the alternative models to generate similar growth trajectories as described in *Model validation and analysis*.

First, a simple allometric model was considered as plausible alternative for ΔL_b:

$$\Delta L_b = \alpha d_b^{\beta} \quad (5)$$

Second, we used the empirical model underlying the statistics in Table 2 of Lintunen and Kaitaniemi (2010) to infer ΔL_b from the statistical model explaining variation in growth vigour (GV). Lintunen and Kaitaniemi (2010) measured GV as $totlong_t/totlength_{t-1}$, where $totlong_t$ is the measured total annual elongation at the end of year t and $totlength_{t-1}$ is the total length (including all alive side branches) at the end of year t-1. Since GV in Lintunen and Kaitaniemi (2010) was based on tree level sums of lengths, including stem elongation, we assumed that the individual branches grew with the same GV as whole trees, resulting in

$$GV = 0.13 + p_1 - 0.003 \times treeage + p_2 \times CI_{12} - 0.014 \times treeage \times CI_{12} \quad (6)$$

$$\Delta L_b\ (t) = GV \times L_t\ (t\text{-}1)$$

where CI_{12} is a competition index, $p_1 = 0.03$ and $p_2 = 0.02$ with Scots pine neighbours, and $p_1 = 0$ and $p_2 = 0.03$ with silver birch neighbours. The measured values of input variables (Lintunen and Kaitaniemi, 2010) were used in the analysis of ΔL_b whereas the generation of growth trajectories relied on the average GV observed in the

data.

Third, the model predicting ΔL_s and underlying the statistics in Lintunen and Kaitaniemi (2010) was also applied to the subset of trees and shoots present in our sample

$$\Delta L_s = 1.18 - 23.3 \times CI_9 - 0.27 \times treeage + 0.02 \times h_{rc} + 0.005 L_c + 0.0005 \times h_{rc} \times L_c + 0.91 \times CI_9 \times treeage + p_1 + p_2 \times CI_9 + p_3 \times treeage + p_4 + p_5 \times h_{rc} \quad (7)$$

where CI_9 is a competition index, L_c is equal to l_b, $p_1 = 0$, $p_2 = 0$ and $p_3 = 0$ with silver birch neighbours, $p_1 = 0.86$, $p_2 = -0.51$ and $p_3 = -0.06$ with Scots pine neighbours, p_4 varies as a function of i as $p_{4(1)} = 3.4$, $p_{4(2)} = 3.6$, $p_{4(3)} = 3.9$ and $p_{4(4)} = 3.3$ with $p_{4(1)}$ being the parameter for primary branch etc, and p_5 correspondingly varies as a function of i as $p_{5(1)} = 0.18$, $p_{5(2)} = 0.04$, $p_{5(3)} = -0.05$ and $p_{5(4)} = -0.01$. The generation of crown profile, by predicting the ΔL_s of the primary branch, was based on the observed average values of CI_9 and *treeage* and the assumption of silver birch neighbours (Lintunen and Kaitaniemi, 2010). The values of h_{rc} and L_c for the generation of crown profile were calculated as described in Appendix A.

Eqs. (6) and (7) both describe statistical models with interactions between continuous variables, which requires the values predicted to be calculated as described, e.g. in Jaccard et al. (1990). We used the SAS procedure GENMOD to generate the predicted values as an output.

3. Results

3.1. Performance with calibration data

The variables X_i retained in the final model for total branch elongation ΔL_b (Table 3a) included the height of branch base in relation to crown length (h_{rc}), branch base diameter (d_b), and branch-specific average values of both relative distance of long shoots from branch base along the main axis ($l_{rb,\ av}$) and side branch diameter at bifurcation points ($d_{s,\ av}$). The final model for individual long shoot elongation ΔL_s (Table 3b) also included the height of branch base in relation to crown length (h_{rc}) and branch base diameter (d_b), together with the diameter at the bifurcation point of the side branch bearing the long shoot (d_s).

The model in Table 3a predicted ΔL_b with higher precision (Table 4, Fig. 2a) than the model of eq. (6), in which a constant *GV* throughout the crown was assumed (Table 4, Fig. 2b). The fit of the allometric eq. (5) with respect to ΔL_b was also inadequate (Table 4, Fig. 2c). The model in Table 3b predicted ΔL_s slightly better (Table 4, Fig. 3a) than eq. (7) (Table 4, Fig. 3b).

3.2. Performance with validation data

The model of ΔL_b produced a growth trajectory for L_t that was closely similar to both the trajectory of total branch length observed in the field (Fig. 4a), and the trajectory for branch biomass resulting from the model by Tahvanainen and Forss (2008) (Fig. 4b). Predictions based on GV in eq. (6) failed to follow the observed values. The simple allometric model of eq. (5) (with parameters $\alpha = 38.4$, $\beta = 0.26$) succeeded well in predicting L_t, although it did not track the curvilinear trajectories predicted by both the model of ΔL_b and Tahvanainen and Forss (2008) (Fig. 4).

The model of ΔL_s applied to predict the growth trajectory of the branch main axis resulted in an approximate crown profile that followed the observed branch lengths, whereas the model in eq. (7) overestimated branch lengths (Fig. 5).

Table 3
Final variables and parameter values (± 95 % confidence interval) in the power-law models constructed to describe a) total branch elongation and b) individual long shoot elongation.

α	$g1$	$g2$	$g3$	$g4$
a) $\Delta L_b = \alpha h_{rc}^{g1} l_{rb,av}^{g2} d_b^{g3} d_{s,av}^{g4}$				
10.7 ± 8.5	1.5 ± 0.6	−0.8 ± 0.3	1.4 ± 0.3	−1.1 ± 0.5
b) $\Delta L_s = \alpha h_{rc}^{g1} d_s^{g2} d_b^{g3}$				
36.2 ± 6.0	1.0 ± 0.9	0.9 ± 0.2	−0.6 ± 0.2	

Table 4
The Bayesian Information Criterion (BIC) for the corresponding model, and the intercept and slope of the regression between the observed vs. the predicted values for the alternative models of a) total branch elongation (Fig. 2) and b) individual long shoot elongation (Fig. 3). Significance tests for the regression parameters given as * $P \leq 0.05$ and *** $P \leq 0.001$.

		BIC	Intercept	Slope
a) ΔL_b				
	Table 3a	1434.8	0.1	1.0***
	Eq. (5)	1524.7	–10.6	1.3*
	Eq. (6)	1922.3	31.8***	0.2*
b) ΔL_s				
	Table 3b	2071.5	0.4	1.0***
	Eq. (7)	2134.3	–1.4	1.4***

3.3. Model predictions

The parameter values in the final models (Table 3) suggest that h_{rc} and d_b both have a strong effect on ΔL_b (Table 3a). Further, ΔL_b was highest in branches with low branch-specific average side branch diameter at the bifurcation points within a branch ($d_{s,av}$) and low branch-specific average distance of shoots from the branch base along the main chord ($l_{rb,av}$). ΔL_s increased with increasing h_{rc} and decreased as a function of d_b (Table 3b). High d_s was associated with increased ΔL_s.

The graphical plots showed an increase in ΔL_b (Table 3a) towards the crown apex and as a function of branch diameter (Fig. 6a). ΔL_b was highest in branches that showed the lowest $d_{s,av}$ values and which had most of their shoots close to the branch base (Fig. 6b).

ΔL_s (Table 3b) increased towards the crown apex and decreased as a function of d_b (Fig. 7a). High values of d_s were associated with increased ΔL_s (Fig. 7b).

4. Discussion

4.1. Model-predicted crown features

The model-predicted trajectories of long-term branch elongation were capable of reproducing the dynamic development of crown profile and the accumulation of branch length and biomass in the course of tree growth, which are features not addressed by typical static crown profile models (Power et al., 2012; Crecente-Campo et al., 2013; Gao et al., 2017). At the same time, the models served as construction rules applicable throughout entire silver birch crowns and they predicted many non-trivial features of crown formation, which previously have been reported in various species and in separate studies. The models reproduced a higher growth rate towards the tree apex in terms of both ΔL_b (Goulet et al., 2000; Colombo and Templeton, 2006) and ΔL_s (Remphrey et al., 2002, Takahashi et al., 2006), the decrease in ΔL_b and ΔL_s in the lowest branches (Goulet et al., 2000; Umeki and Kikuzawa, 2000), the effect of branching order (measured here as d_s) on ΔL_s (Kozlowski and Ward, 1961) and the higher values in the ΔL_b of thick branches in comparisons using equal branch height (Goulet et al., 2000).

Within-crown accumulation of branch biomass, estimated as the total length of the woody branch parts, was closely similar to the growth trajectory based on direct biomass measures (Tahvanainen and

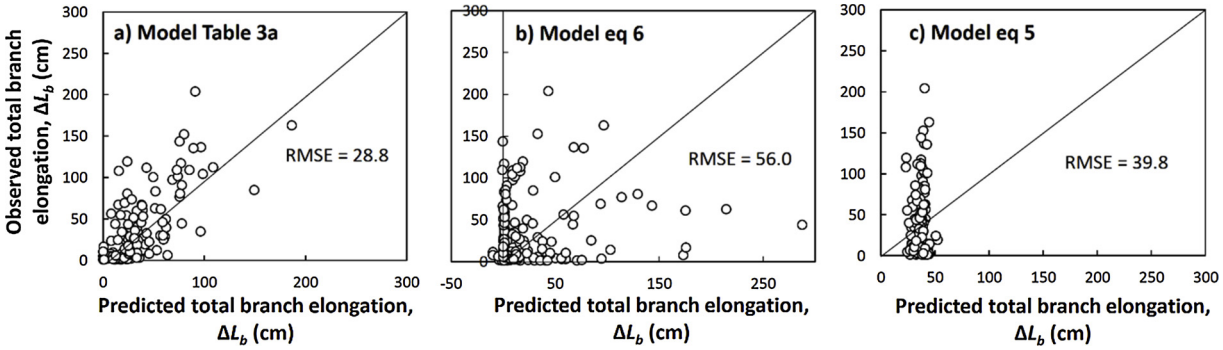

Fig. 2. Plots with observed vs. predicted total branch elongation (ΔL_b) using different models. The 1:1 lines are also shown.

Forss, 2008). The model of ΔL_b appeared to slightly overestimate L_t in comparison with the field observations, which may result from the exclusion of dead side branches in the measurements of L_t in the field.

4.2. Model performance

The predicted crown profile corresponded to measurements of branch length and was comparable to our previous architectural model (Lintunen et al., 2011). However, the predicted L_c of the longest primary branches remained below the approximate 3-m maximum reported for mature silver birch (Ilomäki et al., 2003; Sellin and Kupper, 2006), and observed also in the largest crowns of our data. In part this may reflect the effects of stand density on crown development (Ilomäki et al., 2003), hence potentially on the model parameters as well, but may also reflect the unknown consequences of using the growth measurements of just a single year for model parameterization. Similarly, the largest crowns in our data had also considerably higher L_t than that predicted by the model, which suggests the need for caution in applying the model to tree and stand conditions not typical for our data.

The crown profile and the resulting final branch length predicted by our models was also sensitive to the effect of d_s, which we estimated simply by assuming a taper model common for all branch positions. Thus, the model precision can probably be improved by using refined values for d_s and by re-estimating its associated parameter *g2*.

Overall, the new models were simpler than our previous model versions and provided reasonably good fit, considering the wide size range and geographical distribution of the sample trees. The amount of variation in growth of birch individuals can be large even in far more strictly defined tree samples (Umeki and Kikuzawa, 2000; Umeki and Seino, 2003).

4.3. Modelling processes of crown construction

We consider the dynamic nature of the models as an important step towards incorporating the actual crown construction processes in applications that utilize the structural features of crown shape. An efficient tool in the process is the selection of variables for the final models, which acts as a procedure for identifying key factors that modify branch growth. A striking feature of the final models was that they operated with morphological variables that are measurable by hand, or currently perhaps using terrestrial laser scanning (Raumonen et al., 2015; Sievänen et al., 2018). The predictable behaviour of the models suggests that morphological measurements for estimating the amount of annual growth together with power-law approximation can be successfully used to analyse and construct models that capture many essential features of actual growth processes.

In contrast to purely stochastic tree clones generated from laser scanning data (Potapov et al., 2016; 2017), power-law models can provide insight into physiological processes, because they can easily be refined to include and assess the importance of additional physiological factors. In contrast to a more traditional approach, in which a separate model is used to calculate the amount of resources and empirical growth rules are used to generate crown architecture (Renton et al., 2005b), the power-law approach demonstrated its capability for dynamic generation of realistic crown features on its own.

It was also evident that the simple allometric model, in which the normalization constant was included as a single variable without any spatial information, was inadequate to predict the variability of growth in individual branches. Even though the allometric model reasonably followed the average growth trajectory of branches, it failed to depict the slowing-down of branch growth towards the crown base (Maillette, 1982). Thus, the power-law models provided improved features compared to the simple allometric model, and also served as a tool for

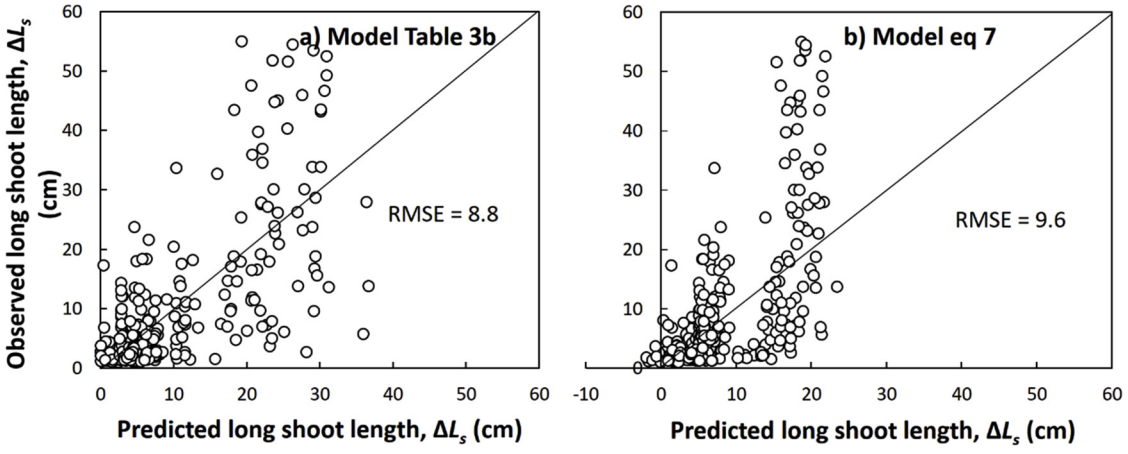

Fig. 3. Plots with observed vs. predicted individual long shoot length (ΔL_s) using different models. The 1:1 lines are also shown.

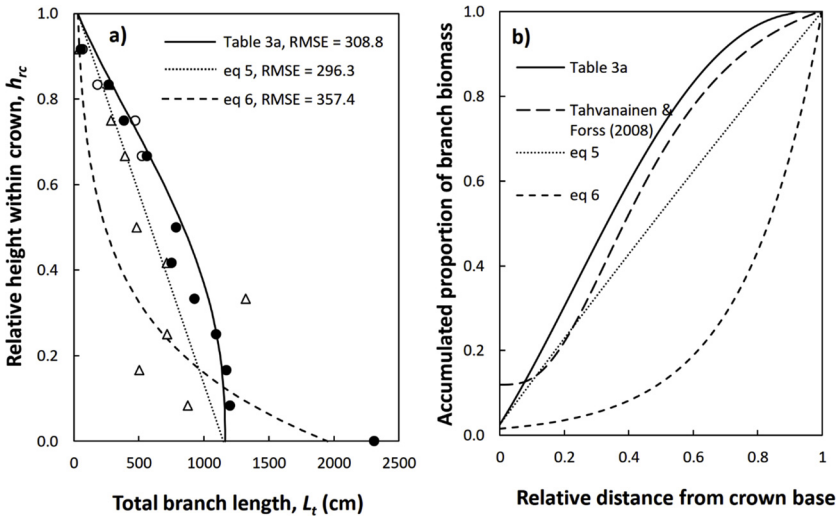

Fig. 4. a) Growth trajectories for the total length of all woody branch parts predicted by the models Table 3a (black line), eq. (5) (dotted line) and eq. (6) (short dashes). The symbols indicate average observed total branch length in three tree age classes (white circle is below 10, triangle is 10–20, and black circle is above 20 years). Branch age was used to estimate a standardized h_{rc} for the observed branch length in different tree age classes (see Appendix A). b) Cumulative total length of all woody branch parts in relation to the maximum total branch length predicted by the models in a), and compared with the model of proportional cumulative biomass (Tahvanainen and Forss, 2008) at different values of h_{rc} (long dashes). A new branch is initiated at lower left and reaches its maximum size at upper right.

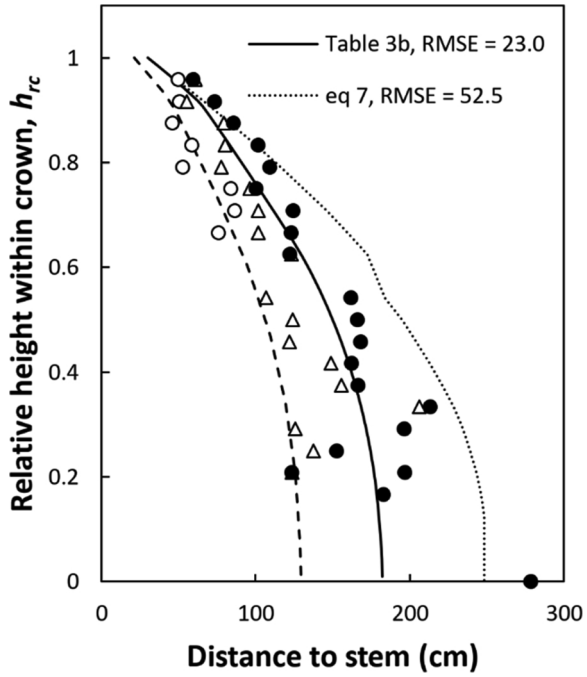

Fig. 5. Growth trajectories of a primary branch axis predicted by the models Table 3b (black line) and eq. (7) (dotted line), illustrated as the distance from the branch tip to the stem, together with an approximate crown profile (dashed line) estimated from the trajectory of axis length predicted by model Table 3b. Growth of a single primary branch axis was predicted as its h_{rc} decreases during stem elongation. A 90° branching angle was used in the plots for growth trajectories, and a 45° branching angle in the plot of crown profile. The symbols indicate average observed primary branch axis length in three tree age classes (white circle is below 10, triangle is 10–20, and black circle is above 20 years). Branch age was used to estimate a standardized h_{rc} for the observed branch length in different tree age classes as explained in Appendix A.

assessing factors that may influence the values of constituents in allometric equations and their patterns of covariation. The values of the scaling exponent and normalization constant are tightly linked, and various combinations of values may provide acceptable fit with empirical observations (West and West, 2011). Analysing power-law models with or without assuming a constant scaling exponent can be used to reveal information on processes that generate variation in empirically observed scaling relationships (Kaitaniemi and Lintunen, 2008).

A useful future enhancement would be the addition or replacement of driving X_i variables using variables that directly indicate the resources available for crown development. A more explicit consideration of the branching topology and the sequence of events during crown and stand development may also be beneficial, because various mechanisms can contribute to growth at different crown positions and at different times of tree ontogeny. At the crown apex, the availability of light may guide upward growth sufficient for a tree to persist in competition, although at some point hydraulic constraints will limit the increase in height (Ishii et al., 2008). At lower crown positions, dynamically changing differences in relative shading (Henriksson, 2001), amount of growing space (Jones and Harper, 1987), branch orientation in relation to the sun (Stoll and Schmid, 1998), GV, and timing of events (Duchesneau et al., 2001) may be more influential and give rise to other typical responses, such as crown asymmetry. The costs of maintenance are likely to increase as branch size increases (Cannell and Morgan, 1989; Spatz and Bruechert, 2000), and the longest and most vigorous branches can also become subject to mechanical abrasion with neighbouring trees, both setting limits to branch growth and GV (Hajek et al., 2015; Loehle, 2016). Since neighbouring trees and other biotic factors undergo simultaneous changes, crown structure is likely to be rarely at the fully optimal state.

Since we did not detect the effect of neighbour distance on branch growth, the distance to neighbouring trees may have occurred over a range in which a change in distance itself does not explain crown expansion (Simard and Zimonick, 2005). The stand densities were relatively low (Lintunen and Kaitaniemi, 2010), and extensive mechanical contacts generating prominent crown asymmetry were not anticipated or observed. We also used an average measure of distance for all the basal branches throughout the crown, whereas mechanical contacts may be prominent only in specific compass directions and in the longest branches (Hajek et al., 2015).

The list of explanatory variables in the final models included indirect factors such as d_s, h_{rc} and $l_{rb,\ av}$, whereas some direct factors were omitted, such as PAR and N_{area}, which indicate potential photosynthetic capacity within the crown. The exclusion of PAR and N_{area} suggests that the indirect variables defining mainly the relative position of the branches and shoots within the crown were sufficient to capture the effect of PAR and N_{area}. There are several examples of positional effects in addition to light that can influence growth responses, and the use of d_s, h_{rc} and $l_{rb,\ av}$ may have indicated the favourability of growth positions relative to the structural organization of the entire crown. For example, differences in the relative levels of shading instead of absolute differences in PAR may greatly modify the allocation of growth (Henriksson, 2001; Dong et al., 2015), while differences in height or GV

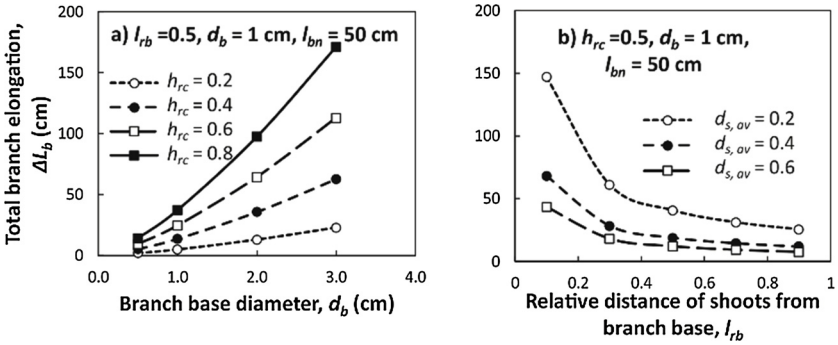

Fig. 6. Effect of selected variables in the model in Table 3a on total branch elongation (ΔL_b). Other variables were set to constant values shown inside the figures.

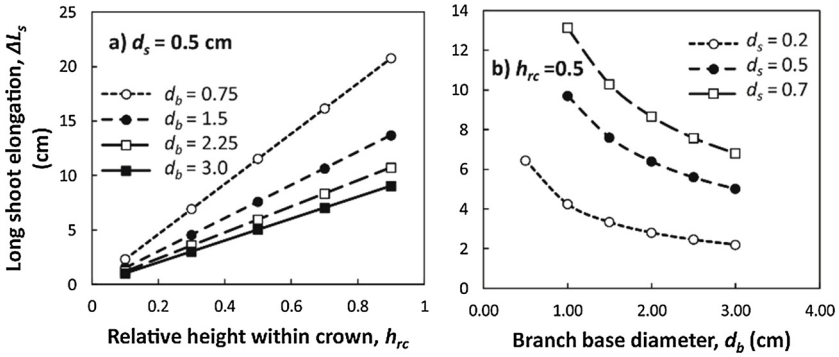

Fig. 7. Effect of selected variables in the model in Table 3b on individual long shoot elongation (ΔLs). Other variables were set to constant values shown inside the figures.

among branches may affect growth independently of light (Goulet et al., 2000, Osada et al., 2014), and mechanisms of apical control may also contribute to growth allocation (Duchesneau et al., 2001, Palubicki et al., 2009).

The use of d_s, h_{rc} and $l_{rb,\,av}$ as indirect explanatory variables in the models can be considered as a shortcut to cover multiple possible configurations of internal organization, although there may remain the need for more precise definition through the specification and inclusion of additional factors X_i in the models. However, many alternative trait configurations may provide plants with equal performance in terms of growth or other measures of success (Delagrange et al., 2004; Hubbell, 2006; Marks and Lechowicz, 2006; Kaitaniemi, 2007), thus even a simplified model can be operationally efficient for many purposes (Rosindell et al., 2012).

Some important factors were omitted from the models for reasons of simplicity or lack of sufficient data. For example, temperature, precipitation and site fertility greatly influence tree growth (Niinemets and Lukjanova, 2003; Dewar et al., 2009), and in models where prediction at multiple locations and for several years is required, they are clearly candidates to be included with their own X_i as driving variables to indicate the availability of resources for growth. Investment in reproduction or losses to herbivory could be included as an efflux that removes resources from growth. We also ignored the effects of neighbouring species and competition indices, which we previously reported as being influential for silver birch growth and crown construction (Lintunen and Kaitaniemi, 2010). Instead, they were considered through the use of PAR and N_{area}, both of which increase with the presence of silver birch as the dominant neighbouring species in comparison to Scots pine neighbours with equal height (Kaitaniemi et al., 2018). The positional variables d_s, h_{rc} and l_{rb} may have incorporated the direct effects of PAR and N_{area}.

5. Conclusions

We conclude that the power-law approach shows good potential for modelling and analysing crown development at the level of 3D crown structure, using variables that capture features of both structure and functioning of crowns. The models can provide improved precision regarding allocation of growth compared with classical statistical models or simple allometric estimates of growth. Even further precision may be obtained by including resource availability and identifying the consequences of processes associated with detailed branching topology and spatial interactions among trees during stand development.

Declaration of Competing Interest

None.

Acknowledgment

We thank P. Schiestl-Aalto and two anonymous referees for their valuable suggestions.

Appendix A. Supplementary data

Supplementary material related to this article can be found, in the online version, at doi:https://doi.org/10.1016/j.ecolmodel.2019.108900.

References

Baldwin Jr., V.C., Peterson, K.D., 1997. Predicting the crown shape of loblolly pine trees. Can. J. For. Res. 27, 102–107.

Baraldi, R., Rossi, F., Facini, O., Fasolo, F., Rotondi, A., Magli, M., Nerozzi, F., 1994. Light environment, growth and morphogenesis in a peach tree canopy. Physiol. Plantarum 91, 339–345.

Bejan, A., Lorente, S., Lee, J., 2008. Unifying constructal theory of tree roots, canopies and forests. J. Theor. Biol. 254, 529–540.

Bentley, L.P., Stegen, J.C., Savage, V.M., Smith, D.D., von Allmen, E.I., Sperry, J.S., Reich, P.B., Enquist, B.J., 2013. An empirical assessment of tree branching networks and implications for plant allometric scaling models. Ecol. Lett. 16, 1069–1078.
Brüchert, F., Gardiner, B., 2006. The effect of wind exposure on the tree aerial architecture and biomechanics of Sitka spruce (*Picea sitchensis*, Pinaceae). Am. J. Bot. 93, 1512–1521.
Buck-Sorlin, G.H., 2000. Models of crown architecture in *Quercus petraea* and *Q. robur*: shoot lengths and bud numbers. Forestry 73, 1–19.
Cannell, M.G.R., Morgan, J., 1989. Branch breakage under snow and ice loads. Tree Physiol. 5, 307–317.
Chen, L., Sumida, A., 2017. Patterns of branch growth and death in crowns of Sakhalin spruce, *Picea glehnii* (F. Schmidt). Mast. Forests 8, 26.
Coble, A.P., Fogel, M.L., Parker, G.G., 2017. Canopy gradients in leaf functional traits for species that differ in growth strategies and shade tolerance. Tree Physiol. 37, 1415–1425.
Cole, W.G., Lorimer, C.G., 1994. Predicting tree growth from crown variables in managed northern hardwood stands. For. Ecol. Manage. 67, 159–175.
Collet, C., Fournier, M., Ningre, F., Hounzandji, A.P.-I., Constant, T., 2011. Growth and posture control strategies in *Fagus sylvatica* and *Acer pseudoplatanus* saplings in response to canopy disturbance. Ann. Bot. 107, 1345–1353.
Colombo, S.J., Templeton, C.W.G., 2006. Bud and crown architecture of white spruce and black spruce. Trees 20, 633–641.
Crecente-Campo, F., Alvarez-Gonzalez, J.G., Castedo-Dorado, F., Gomez-Garcia, E., Dieguez-Aranda, U., 2013. Development of crown profile models for *Pinus pinaster* Ait., *Pinus sylvestris* L. In northwestern Spain. Forestry 86, 481–491.
Delagrange, S., Messier, C., Lechowicz, M.J., Dizengremel, P., 2004. Physiological, morphological and allocational plasticity in understory deciduous trees: importance of plant size and light availability. Tree Physiol. 24, 775–784.
Dewar, R.C., Franklin, O., Mäkelä, A., McMurtrie, R.E., Valentine, H.T., 2009. Optimal function explains forest responses to global change. BioScience 59, 127–139.
Dong, T., Li, J., Zhang, Y., Korpelainen, H., Niinemets, Ü., Li, C., 2015. Partial shading of lateral branches affects growth, and foliage nitrogen- and water-use efficiencies in the conifer *Cunninghamia lanceolata* growing in a warm monsoon climate. Tree Physiol. 35, 632–643.
Duchesneau, R., Lesage, I., Messier, C., Morin, H., 2001. Effects of light and intraspecific competition on growth and crown morphology of two size classes of understory balsam fir saplings. For. Ecol. Manage. 140, 215–225.
Enquist, B.J., 2002. Universal scaling in tree and vascular plant allometry: toward a general quantitative theory linking plant form and function from cells to ecosystems. Tree Physiol. 22, 1045–1064.
Evans, J.R., 1989. Photosynthesis and nitrogen relationships in leaves of C3 plants. Oecologia 78, 9–19.
Farnsworth, K.D., Niklas, K.J., 1995. Theories of optimization, form and function in branching architecture in plants. Funct. Ecol. 9, 355–363.
Ford, E.D., 2014. The dynamic relationship between plant architecture and competition. Front. Plant Sci. 5, 1–13.
Ford, E.D., Avery, A., Ford, R., 1990. Simulation of branch growth in the *Pinaceae*: interactions of morphology, phenology, foliage productivity and the requirement for structural support on the export of carbon. J. Theor. Biol. 146, 15–36.
Gao, H., Bi, H., Li, F., 2017. Modelling conifer crown profiles as nonlinear conditional quantiles: an example with planted Korean pine in northeast China. For. Ecol. Manage. 398, 101–115.
Gendron, F., Messier, C., Comeau, P.G., 1998. Comparison of various methods for estimating the mean growing season percent photosynthetic photon flux density in forests. Agr. Forest Meteorol. 92, 55–70.
Gonda-King, L., Gomez, S., Martin, J.L., Orians, C.M., Preisser, E.L., 2014. Tree responses to an invasive sap-feeding insect. Plant Ecol. 215, 297–304.
Goulet, J., Messier, C., Nikinmaa, E., 2000. Effect of branch position and light availability on shoot growth of understory sugar maple and yellow birch saplings. Can. J. Bot. 78, 1077–1085.
Grote, R., Pretzsch, H., 2002. A model for individual tree development based on physiological processes. Plant Biol. 4, 167–180.
Grönlund, L., Hölttä, T., Mäkelä, A., 2016. Branch age and light conditions determine leaf-area-specific conductivity in current shoots of Scots pine. Tree Physiol. 36, 994–1006.
Hajek, P., Seidel, D., Leuschner, C., 2015. Mechanical abrasion, and not competition for light, is the dominant canopy interaction in a temperate mixed forest. For. Ecol. Manage. 348, 108–116.
Haukioja, E., Ruohomäki, K., Senn, J., Suomela, J., Walls, M., 1990. Consequences of herbivory in the mountain birch (*Betula pubescens* ssp *tortuosa*): importance of the functional organization of the tree. Oecologia 82, 238–247.
Henriksson, J., 2001. Differential shading of branches or whole trees: survival, growth, and reproduction. Oecologia 126, 482–486.
Hubbell, S.P., 2006. Neutral theory and the evolution of ecological equivalence. Ecology 87, 1387–1398.
Ilomäki, S., Nikinmaa, E., Mäkelä, A., 2003. Crown rise due to competition drives biomass allocation in silver birch. Can. J. For. Res. 33, 2395–2404.
Ishii, H.T., Jennings, G.M., Sillett, S.C., Koch, G.W., 2008. Hydrostatic constraints on morphological exploitation of light in tall *Sequoia sempervirens* trees. Oecologia 156, 751–763.
Jaccard, J., Wan, C.K., Turrisi, R., 1990. The detection and interpretation of interaction effects between continuous variables in multiple regression. Multivar. Behav. Res. 25, 467–478.
James, K.R., Haritos, N., Ades, P.K., 2006. Mechanical stability of trees under dynamic loads. Am. J. Bot. 93, 1522–1530.
Jones, M., Harper, J.L., 1987. The influence of neighbours on the growth of trees: II. The fate of buds on long and short shoots in *Betula pendula*. Proc. R. Soc. B 232, 19–33.
Kaitaniemi, P., 2007. Consequences of variation in tree architecture and leaf traits on light capture and photosynthetic nitrogen use efficiency in mountain birch. Arct. Antarct. Alp. Res. 39, 258–267.
Kaitaniemi, P., Lintunen, A., 2010. Neighbor identity and competition influence tree growth in Scots pine, Siberian larch, and silver birch. Ann. For. Sci. 67 604–604.
Kaitaniemi, P., Lintunen, A., 2008. Precision of allometric scaling equations for trees can be improved by including the effect of ecological interactions. Trees 22, 579–584.
Kaitaniemi, P., Lintunen, A., Sievänen, R., 2018. Computational analysis of the effects of light gradients and neighbouring species on foliar nitrogen. Ecol. Informatics 48, 171–177.
Kantola, A., Mäkelä, A., 2004. Crown development in Norway spruce [*Picea abies* (L.) Karst.]. Trees 18, 408–421.
Koch, G.W., Sillett, S.C., Jennings, G.M., Davis, S.D., 2004. The limits to tree height. Nature 428, 851–854.
Koyama, K., Yamamoto, K., Ushio, M., 2017. A lognormal distribution of the lengths of terminal twigs on self-similar branches of elm trees. Proc. R. Soc. B 284, 20162395.
Kozlowski, T.T., Ward, R.C., 1961. Shoot elongation characteristics of forest trees. For. Sci. 7, 357–368.
Kramer, R.D., Sillett, S.C., Carroll, A.L., 2014. Structural development of redwood branches and its effects on wood growth. Tree Physiol. 34, 314–330.
Kukk, M., Sõber, A., 2015. Bud development and shoot morphology in relation to crown location. AoB Plants 7 plv082.
Kull, O., Tulva, I., 2002. Shoot structure and growth along a vertical profile within a *Populus-Tilia* canopy. Tree Physiol. 22, 1167–1175.
Lacointe, A., 2000. Carbon allocation among tree organs: a review of basic processes and representation in functional-structural tree models. Ann. For. Sci. 57, 521–533.
Lines, E.R., Zavala, M.A., Purves, D.W., Coomes, D.A., 2012. Predictable changes in aboveground allometry of trees along gradients of temperature, aridity and competition: predictable variation in tree aboveground allometry. Global Ecol. Biogeogr. 21, 1017–1028.
Lintunen, A., 2013. Crown Architecture and Its Role in Species Interactions in Mixed Boreal Forests. Dissertation. University of Helsinki.
Lintunen, A., Kaitaniemi, P., 2010. Responses of crown architecture in *Betula pendula* to competition are dependent on the species of neighbouring trees. Trees 24, 411–424.
Lintunen, A., Sievänen, R., Kaitaniemi, P., Perttunen, J., 2011. Models of 3D crown structure for Scots pine (*Pinus sylvestris*) and silver birch (*Betula pendula*) grown in mixed forest. Can. J. For. Res. 41, 1779–1794.
Lintunen, A., Kaitaniemi, P., Perttunen, J., Sievänen, R., 2013. Analysing species-specific light transmission and related crown characteristics of *Pinus sylvestris* and *Betula pendula* using a shoot-level 3D model. Can. J. For. Res. 43, 929–938.
Loehle, C., 2016. Biomechanical constraints on tree architecture. Trees 30, 2061–2070.
Maillette, L., 1982. Structural dynamics of Silver birch I. The fates of buds. J. Appl. Ecol. 19, 203–218.
Marks, C.O., Lechowicz, M.J., 2006. Alternative designs and the evolution of functional diversity. Am. Nat. 167, 55–66.
Mathieu, A., Cournède, P.H., Letort, V., Barthélémy, D., de Reffye, P., 2009. A dynamic model of plant growth with interactions between development and functional mechanisms to study plant structural plasticity related to trophic competition. Ann. Bot. 103, 1173–1186.
Messier, C., Nikinmaa, E., 2000. Effects of light availability and sapling size on the growth, biomass allocation, and crown morphology of understory sugar maple, yellow birch, and beech. Ecoscience 7, 345–356.
Mäkinen, H., 2002. Effect of stand density on the branch development of silver birch (*Betula pendula* Roth) in central Finland. Trees 16, 346–353.
Nakamura, M., Makoto, K., Tanaka, M., Inoue, T., Son, Y., Hiura, T., 2016. Leaf flushing and shedding, bud and flower production, and stem elongation in tall birch trees subjected to increases in aboveground temperature. Trees 30, 1535–1541.
Niinemets, Ü., Lukjanova, A., 2003. Needle longevity, shoot growth and branching frequency in relation to site fertility and within-canopy light conditions in *Pinus sylvestris*. Ann. For. Sci. 60, 195–208.
Normand, F., Bello, A.K.P., Trottier, C., Lauri, P.-É., 2009. Is axis position within tree architecture a determinant of axis morphology, branching, flowering and fruiting? An essay in mango. Ann. Bot. 103, 1325–1336.
Obeso, J.R., 1997. Costs of reproduction in *Ilex aquifolium*: effects at tree, branch and leaf levels. J. Ecol. 85, 159.
Osada, N., Okabe, Y., Hayashi, D., Katsuyama, T., Tokuchi, N., 2014. Differences between height- and light-dependent changes in shoot traits in five deciduous tree species. Oecologia 174, 1–12.
Palubicki, W., Horel, K., Longay, S., Runions, A., Lane, B., Měch, R., Prusinkiewicz, P., 2009. Self-organizing tree models for image synthesis. ACM T Graphic 28, 1.
Peters, R., Olagoke, A., Berger, U., 2018. A new mechanistic theory of self-thinning: adaptive behaviour of plants explains the shape and slope of self-thinning trajectories. Ecol. Modelling 390, 1–9.
Piñeiro, G., Perelman, S., Guerschman, J.P., Paruelo, J.M., 2008. How to evaluate models: observed vs. predicted or predicted vs. observed? Ecol. Model. 216, 316–322.
Potapov, I., Järvenpää, M., Åkerblom, M., Raumonen, P., Kaasalainen, M., 2016. Data-based stochastic modeling of tree growth and structure formation. Silva Fenn. 50, 1–11.
Potapov, I., Järvenpää, M., Åkerblom, M., Raumonen, P., Kaasalainen, M., 2017. Bayes forest: a data-intensive generator of morphological tree clones. GigaScience 6, 1–13.
Power, H., LeMay, V., Berninger, F., Sattler, D., Kneeshaw, D., 2012. Differences in crown characteristics between black (*Picea mariana*) and white spruce (*Picea glauca*). Can. J. For. Res. 42, 1733–1743.
Pretzsch, H., 2014. Canopy space filling and tree crown morphology in mixed-species stands compared with monocultures. For. Ecol. Manage. 327, 251–264.

Raumonen, P., Casella, E., Calders, K., Murphy, S., Åkerblom, M., Kaasalainen, M., 2015. Massive-scale tree modelling from TLS data. ISPRS annals of photogrammetry, remote sensing and spatial information. Sciences II-3/W4, 189–196.
Remphrey, W.R., Bartlett, G.A., Davidson, C.G., 2002. Shoot morphology and fate of buds in relation to crown location in young *Fraxinus pennsylvanica* var. *subintegerrima*. Can. J. Bot. 80, 1274–1282.
Renton, M., Guédon, Y., Godin, C., Costes, E., 2006. Similarities and gradients in growth unit branching patterns during ontogeny in 'Fuji' apple trees: a stochastic approach. J. Exp. Bot. 57, 3131–3143.
Renton, M., Hanan, J., Burrage, K., 2005a. Using the canonical modelling approach to simplify the simulation of function in functional-structural plant models. New Phytol. 166, 845–857.
Renton, M., Kaitaniemi, P., Hanan, J., 2005b. Functional–structural plant modelling using a combination of architectural analysis, L-systems and a canonical model of function. Ecol. Model. 184, 277–298.
Rosindell, J., Hubbell, S.P., He, F., Harmon, L.J., Etienne, R.S., 2012. The case for ecological neutral theory. Trends Ecol. Evol. 27, 203–208.
Sachs, T., 2004. Self-organization of tree form: a model for complex social systems. J. Theor. Biol. 230, 197–202.
Savage, V.M., Bentley, L.P., Enquist, B.J., Sperry, J.S., Smith, D.D., Reich, P.P., von Allmen, E.I., 2010. Hydraulic trade-offs and space filling enable better predictions of vascular structure and function in plants. Proc. Natl. Acad. Sci. U.S.A. 107, 22722–22727.
Savageau, M.A., 1979a. Allometric morphogenesis of complex systems: derivation of the basic equations from first principles. Proc. Natl. Acad. Sci. U.S.A. 76, 6023–6025.
Savageau, M.A., 1979b. Growth of complex systems can be related to the properties of their underlying determinants. Proc. Natl. Acad. Sci. U.S.A. 76, 5413–5417.
Schwarz, G., 1978. Estimating the dimension of a model. Ann. Stat. 6, 461–464.
Sellin, A., Kupper, P., 2006. Spatial variation in sapwood area to leaf area ratio and specific leaf area within a crown of silver birch. Trees 20, 311–319.
Sievänen, R., Raumonen, P., Perttunen, J., Nikinmaa, E., Kaitaniemi, P., 2018. A study of crown development mechanisms using a shoot-based tree model and segmented terrestrial laser scanning data. Ann. Bot. 122, 423–434.
Sileshi, G.W., 2014. A critical review of forest biomass estimation models, common mistakes and corrective measures. For. Ecol. Manage. 329, 237–254.
Simard, S.W., Zimonick, B.J., 2005. Neighborhood size effects on mortality, growth and crown morphology of paper birch. For. Ecol. Manage. 214, 251–265.
Sone, K., Noguchi, K., Terashima, I., 2006. Mechanical and ecophysiological significance of the form of a young *Acer rufinerve* tree: vertical gradient in branch mechanical properties. Tree Physiol. 26, 1549–1558.
Sorrensen-Cothern, K.A., Ford, E.D., Sprugel, D.G., 1993. A model of competition incorporating plasticity through modular foliage and crown development. Ecol. Monogr. 63, 277–304.
Spatz, H.-C., Bruechert, F., 2000. Basic biomechanics of self-supporting plants: wind loads and gravitational loads on a Norway spruce tree. For. Ecol. Manage. 135, 33–44.
Sprugel, D.G., 2002. When branch autonomy fails: Milton's Law of resource availability and allocation. Tree Physiol. 22, 1119–1124.
Stevenson, M.T., Shackel, K.A., Ferguson, L., 2000. Shoot length distribution and its relation to yield of alternate-bearing pistachio trees. J. Am. Soc. Hortic. Sci. 125, 165–168.
Stoll, P., Schmid, B., 1998. Plant foraging and dynamic competition between branches of *Pinus sylvestris* in contrasting light environments. J. Ecol. 86, 934–945.
Tahvanainen, T., Forss, E., 2008. Individual tree models for the crown biomass distribution of Scots pine, Norway spruce and birch in Finland. For. Ecol. Manage. 255, 455–467.
Takahashi, K., Okada, J.-I., Urata, E., 2006. Relative shoot height and irradiance and the shoot and leaf properties of *Quercus serrata* saplings. Tree Physiol. 26, 1035–1042.
Tworkoski, T., Miller, S., Scorza, R., 2006. Relationship of pruning and growth morphology with hormone ratios in shoots of pillar and standard peach trees. J. Plant Growth Regul. 25, 145–155.
Umeki, K., Seino, T., 2003. Growth of first-order branches in *Betula platyphylla* saplings as related to the age, position, size, angle, and light availability of branches. Can. J. For. Res. 33, 1276–1286.
Umeki, K., Kikuzawa, K., 2000. Patterns in individual growth, branch population dynamics, and growth and mortality of first-order branches of *Betula platyphylla* in northern Japan. Ann. For. Sci. 57, 587–598.
Voit, E.O., 2000. Computational Analysis of Biochemical Systems. Cambridge University Press, Cambridge, UK.
Voit, E.O., Martens, H.A., Omholt, S.W., 2015. 150 years of the mass action law. PLoS Comput. Biol. 11, e1004012.
Voit, E.O., Sands, P.J., 1996. Modeling forest growth II. Biomass partitioning in Scots pine. Ecol. Model. 86, 73–89.
West, D., West, B.J., 2011. Statistical origin of allometry. Europhys. Lett. 94, 38005.
White, J.F., Gould, S.J., 1965. Interpretation of the coefficient in the allometric equation. Am. Nat. 99, 5–18.
Wyka, T.P., Żytkowiak, R., Oleksyn, J., 2016. Seasonal dynamics of nitrogen level and gas exchange in different cohorts of Scots pine needles: a conflict between nitrogen mobilization and photosynthesis? Eur. J. Forest Res. 135, 483–493.
Wolfinger, R.D., 1999. Fitting Non-Linear Mixed Models With the New NLMIXED Procedure. Technical Report. SAS Institute, Cary.
Yoshimura, M., Yamashita, M., 2014. A consideration for the light environmental modeling under tropical rainforest canopies. ISPRS - International Archives of the Photogrammetry. Remote Sensing and Spatial Information Sciences XL-7, 217–220.
Young, T.P., Hubbell, S.P., 1991. Crown asymmetry, treefalls, and repeat disturbance of broad-leaved forest gaps. Ecology 72, 1464–1471.